Published online: January 12, 2016

Article

TRANSPARENT PROCESS

THE EMBO JOURNAL

Microtubule-binding protein doublecortin-like kinase 1 (DCLK1) guides kinesin-3-mediated cargo transport to dendrites

Joanna Lipka[1,2], Lukas C Kapitein[1], Jacek Jaworski[2] & Casper C Hoogenraad[1,*]

Abstract

In neurons, the polarized distribution of vesicles and other cellular materials is established through molecular motors that steer selective transport between axons and dendrites. It is currently unclear whether interactions between kinesin motors and microtubule-binding proteins can steer polarized transport. By screening all 45 kinesin family members, we systematically addressed which kinesin motors can translocate cargo in living cells and drive polarized transport in hippocampal neurons. While the majority of kinesin motors transport cargo selectively into axons, we identified five members of the kinesin-3 (KIF1) and kinesin-4 (KIF21) subfamily that can also target dendrites. We found that microtubule-binding protein doublecortin-like kinase 1 (DCLK1) labels a subset of dendritic microtubules and is required for KIF1-dependent dense-core vesicles (DCVs) trafficking into dendrites and dendrite development. Our study demonstrates that microtubule-binding proteins can provide local signals for specific kinesin motors to drive polarized cargo transport.

Keywords dendrite; doublecortin; kinesin; neuron; polarity
Subject Categories Cell Adhesion, Polarity & Cytoskeleton; Neuroscience
DOI 10.15252/embj.201592929 | Received 26 August 2015 | Revised 2 December 2015 | Accepted 8 December 2015 | Published online 12 January 2016
The EMBO Journal (2016) 35: 302–318

Introduction

Neurons are highly polarized cells that have morphologically and functionally distinct processes called axons and dendrites. To establish and maintain this polarized morphology, efficient targeting mechanisms are required to facilitate compartment-specific cargo delivery. In several model systems, it has been demonstrated that microtubule-dependent kinesin and dynein motors are critically involved in polarized transport and sorting of specific cargo between axons and dendrites (Kapitein & Hoogenraad, 2011; Rolls, 2011). In mammals, a total of 45 kinesin genes have been identified and the majority of kinesins are abundantly present in the brain (Hirokawa *et al*, 2009). These kinesin motors have diverse functions. For instance, members of the kinesin-1, kinesin-2, kinesin-3, and kinesin-4 families are generally thought to function as motors for vesicular transport in neuronal cells (Hirokawa *et al*, 2009). On the other hand, members of the kinesin-8 and kinesin-13 subfamilies are microtubule-depolymerizing kinesins that use their catalytic activities to regulate microtubule dynamics (Walczak *et al*, 2013). Neurons are especially vulnerable to defects in microtubule-based processes: Numerous kinesin motors and their regulators have been implicated in a wide array of neurological and neurodegenerative disorders (Franker & Hoogenraad, 2013; Millecamps & Julien, 2013). However, little is known about the precise role of different kinesin motors in axon and dendritic cargo trafficking.

The specific organization of the neuronal cytoskeleton is critically important for guiding intracellular cargo transport. Microtubule arrays extend along the length of both axons and dendrites, and microtubule-based motor proteins use these cytoskeletal structures to transport cargo to the desired location. Most neuronal microtubules do not emerge from a central microtubule organizing center and their relative orientations vary in axons and dendrites (Stiess & Bradke, 2011; Yau *et al*, 2014). Whereas axonal microtubules are organized such that the plus-end is oriented outward from the cell body, dendrites exhibit a mixed microtubule polarity containing both minus-end- and plus-end-out microtubules (Baas *et al*, 1988). In several model systems, it has been demonstrated that kinesin-1 motors specifically target the axon, whereas the minus-end-directed dynein motor sorts cargo to dendrites (Nakata & Hirokawa, 2003; Zheng *et al*, 2008; Kapitein *et al*, 2010a). However, considering that plus-end-out microtubules are also present in dendrites, it remains unclear whether kinesin family members can also drive cargo transport into dendrites.

Not only the specific microtubule organization in neurons, but also local cues on microtubules may provide selective transport routes for polarized cargo sorting. Axon selectivity appears mediated by specific properties of stabilized axonal microtubules, as treatment with the microtubule stabilizing agent paclitaxel results in non-polarized targeting to both axons and dendrites (Nakata & Hirokawa, 2003; Witte *et al*, 2008; Kapitein *et al*, 2010a). Moreover, there are

1 Cell Biology, Faculty of Science, Utrecht University, Utrecht, The Netherlands
2 Laboratory of Molecular and Cellular Neurobiology, International Institute of Molecular and Cell Biology, Warsaw, Poland
*Corresponding author. Tel: +31 30 2533894; Fax: +31 30 2513655; E-mail: c.hoogenraad@uu.nl

several lines of evidence showing that specific posttranslational modifications (PTMs) can control microtubule-based transport in neurons (Janke, 2014). For instance, kinesin cargo transport is somewhat sensitive for microtubule polyglutamylation, and PTMs influence the motile properties of kinesins on reconstituted microtubules (Ikegami *et al*, 2007; Sirajuddin *et al*, 2014). Microtubule-associated proteins (MAPs) and other microtubule-binding proteins are strongly compartmentalized in neurons and have also been shown to control kinesin motor activity (Atherton *et al*, 2013). For instance, doublecortin (DCX) and doublecortin-like kinase 1 (DCLK1) interact with microtubules and have been implicated in microtubule-based transport processes (Tanaka *et al*, 2004; Liu *et al*, 2012). However, the role of specific microtubule-binding proteins in regulating polarized cargo transport in neurons has not been investigated.

In this study, we systematically determined which of the 45 kinesin family members can translocate cargo in COS-7 cells. We next tested which "cargo translocating" kinesins can drive polarized transport in hippocampal neurons. We found that none of the kinesin motors selectively targets dendrites and that only five members of the kinesin-3 (KIF1A/B/C) and kinesin-4 (KIF21A/B) families can drive transport toward both the axon and dendrites. Moreover, we found that microtubule-binding protein doublecortin-like kinase (DCLK1) specifically localizes to dendrites and is required for kinesin-3-dependent cargo trafficking into dendrites. We propose a model in which DCLK1 at the microtubule surface represents a local regulatory mechanism for KIF1-mediated dendritic cargo transport.

Results

Roughly half of the kinesin motors can transport cargo in living cells

The 45 kinesin superfamily members consist of N-kinesins, C-kinesins, and M-kinesins and are organized into 14 families named kinesin-1 through kinesin-14 (Fig 1A) (Lawrence *et al*, 2004; Hirokawa *et al*, 2010). We first determined which kinesin members can function as motors for active cargo translocation in COS-7 cells. To test for kinesin motor motility, we made use of our previously developed cargo trafficking assay where FRB-FKBP heterodimerization triggers the coupling of kinesin motors to an artificial cargo after the addition of the rapamycin analogue (rapalog, Fig 1B) (Hoogenraad *et al*, 2003; Kapitein *et al*, 2010b). We used stationary peroxisomes as cargos for the read out of the activity of a particular kinesin motor and followed their movement using live-cell imaging. Peroxisomes were labeled by expressing PEX-RFP-FKBP, which is a fusion construct of PEX3, a peroxisomal membrane-targeting signal, the red fluorescent protein (RFP) and FKBP12, a domain that can be bind to FRB in the presence of rapalog (Kapitein *et al*, 2010b). Kinesin constructs were truncated to contain the motor domain and at least one coiled-coil domain (MDC) for dimerization, and fused with FRB and GFP (Fig 1A). Together, 45 KIF-MDC constructs were generated, of which the KIF27-MDC construct was toxic to the cells and therefore omitted from our analysis. In COS-7 cells co-transfected with PEX-RFP-FKBP and KIF-MDC-GFP-FRB constructs, most peroxisomes were immobile and displayed a perinuclear distribution (with a radius ~10 μm near the cell center) before rapalog addition (before, Fig 1C). Treating these cells with rapalog revealed three possible outcomes for the peroxisome distribution; a robust accumulation over time of peroxisomes at the cell periphery (such as KIF1C) or no cargo translocation (such as KIF3B) (after, Fig 1C, see also Movie EV1). The kinesin members were defined as a "cargo translocating" when the peroxisomes moved over a distance of at least 5 μm from their initial position within 30 min after rapalog treatment (Appendix Figs S1 and S2). We found that 23 members of the kinesin superfamily were able to transport peroxisomes in COS-7 cells, of which all are N-kinesins (Fig 1E, Appendix Figs S1 and S2). The cargo translocating kinesins displayed various average dispersion speeds (Fig 1F, Appendix Table S2; note in this analysis that the average dispersion speed does not reflect the actual velocity of a particular motor but is the average speed with which a particular motor translocates cargo from cell center to cell periphery). It should also be noted that truncated kinesin construct that failed in this assay either does not translocate cargos in living cells or misses critical element needed for cargo movement. In contrast, kinesins identified as cargo transporters do not necessarily transport endogenous cargo under physiological conditions. Thus, using the inducible cargo trafficking assay we found that roughly half of the kinesin superfamily members are able to translocate cargo in living cells.

A subset of kinesin-3 and kinesin-4 subfamily members drive cargo transport in both axons and dendrites

We next determined which kinesins can drive polarized transport in hippocampal neurons focusing on those members that transported cargo in COS-7 cells. Fully differentiated hippocampal neurons

Figure 1. Systematic analysis of the transporting properties of kinesin motors.

A Schematic representation of kinesin constructs used in the inducible trafficking assays. Kinesin constructs contain a motor domain and a coil (MDC).

B Principle of inducible peroxisome trafficking assay. COS-7 cells were transfected with truncated motor constructs of kinesins fused with FRB and GFP (summarized in A) and peroxisomes labeled with PEX-mRFP-FKBP. Upon the addition of rapalog, kinesin motors are recruited to peroxisomes, and kinesin transporting features can be measured as peroxisome displacement.

C Exemplary images of COS-7 cells expressing PEX-mRFP-FKBP before (upper panels) and 30 min after (middle panels) rapalog addition in the presence of a translocating motor, KIF1C-MDC-FRB, and a non-translocating motor, KIF3B-MDC-FRB. Yellow lines indicate COS-7 cell outline. Lower panel represents the overlay of sequential binarized images color coded by time (see also Appendix Fig S1). Scale bar, 20 μm.

D Plots representing intensity time traces of R90% for COS-7 cells transfected with PEX-mRFP-FKBP and KIF1C-MDC-FRB (n = 13) or KIF3B-MDC-FRB (n = 10). R90% is the radius for each time point that includes 90% of the total fluorescent intensity. Error bars indicate SEM.

E Quantitative representation of average peroxisome displacement 30 min after the addition of rapalog for COS-7 cells transfected with kinesin constructs summarized in (A). The number of analyzed cells is summarized in Appendix Table S1. Kinesins were considered translocators, if they displaced peroxisomes ≥ 5 μm (marked with a blue dashed line) in 30 min after rapalog addition. Error bars indicate SEM.

F Quantitative representation of average dispersion speed of peroxisomes recruited to translocating kinesins as calculated from time traces of R90% (summarized in Appendix Fig S2, Appendix Table S1). Error bars indicate SEM.

Published online: January 12, 2016
The EMBO Journal

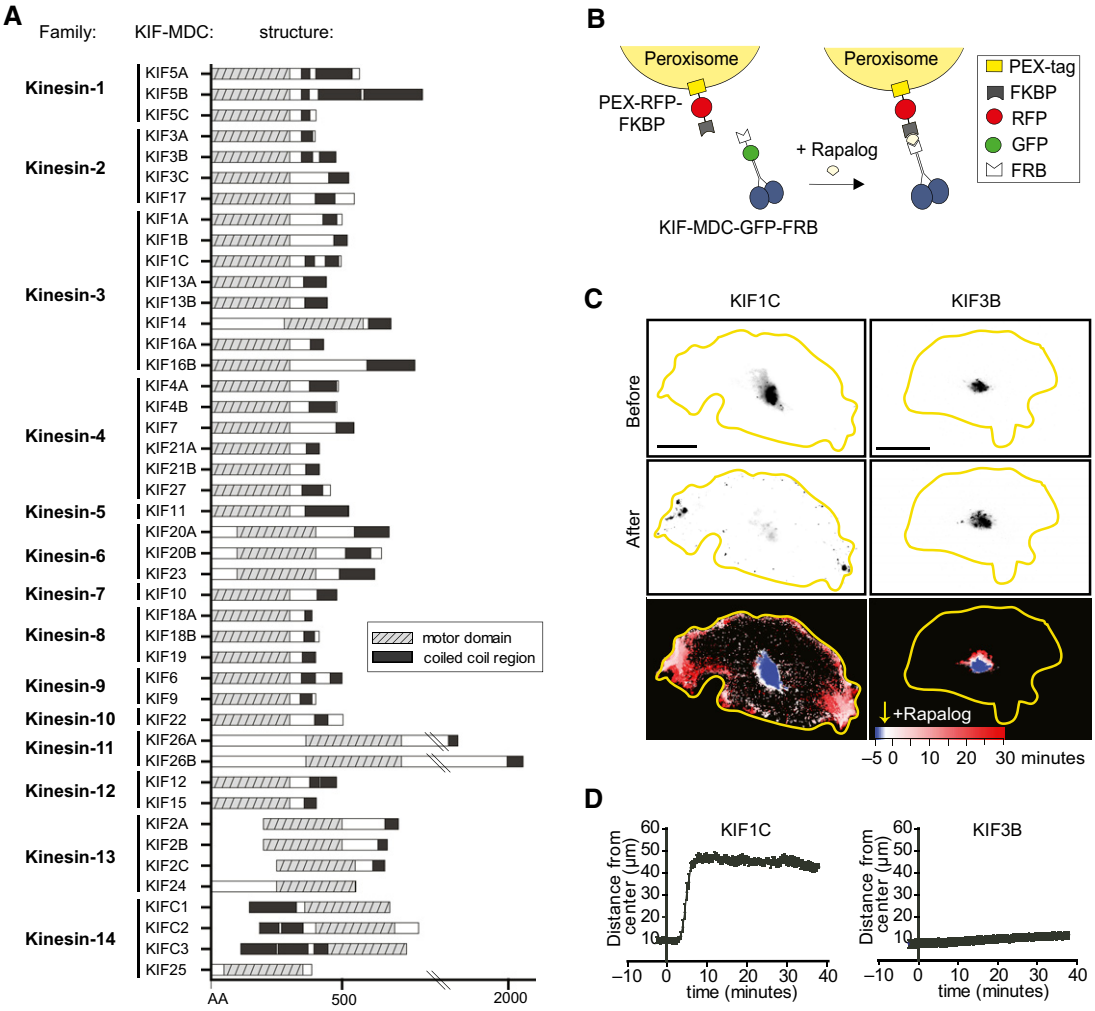

Figure 1.

(stage 5) expressing PEX-RFP-FKBP, KIF-MDC-GFP-FRB, and blue fluorescent protein (BFP), to visualize neuronal morphology, were imaged at 14 days *in vitro* (DIV14) (Fig 2A). At this stage, hippocampal neurons in culture have clearly morphologically distinct axon and dendrites, which can be further discriminated by immunostaining for the axonal marker Tau and dendritic marker MAP2 (Dotti *et al*, 1988; van Spronsen *et al*, 2013b). Consistent with previous results (Kapitein *et al*, 2010a), the addition of rapalog to neurons coexpressing PEX-RFP-FKBP and KIF5B-MDC-GFP-FRB induced a rapid burst of peroxisomes from the cell body into the axon (Fig 2A). No peroxisome movement was observed toward dendrites after KIF5B-MDC-FRB recruitment (Fig 2A). Measuring the PEX-RFP-FKBP intensity changes in axons and dendrites over time directly demonstrated that KIF5B predominantly drives transport into axons (Fig 2B, see also Movie EV2). Kinesins were considered to target dendrites if an increase in the intensity was observed in at least two dendrites in ≥ 50% of the analyzed cells (Fig 2C). All tested kinesin motors drive robust cargo transport into the axon but none of the members selectively target the dendrites (Fig 2C). However, some kinesin members of the same family displayed different targeting preferences. We found that five members of the kinesin-3 (KIF1A, KIF1B, KIF1C) and kinesin-4 (KIF21A and KIF21B) subfamily target peroxisomes to both axons and dendrites (Fig 2A–C, see also Movie EV2), indicating that these five kinesin motors can drive non-polarized cargo transport in neurons. Interestingly, other members of the kinesin-3 (KIF13A, KIF13B, KIF16B) and kinesin-4 (KIF4A, KIF4B) subfamilies selectively drive transport into axons (Fig 2C). These results indicate that highly homologous members of the same subfamily display distinct targeting preferences.

Axon-selective transport has already been observed in developing neurons directly after neuronal polarization (Jacobson *et al*, 2006). We next tested whether KIF1C and KIF21A drive non-polarized cargo transport during the early stages of neuronal development. Hippocampal neurons with developing neurites (stage 2/3) expressing PEX-RFP-FKBP, KIF-MDC-GFP-FRB, and blue fluorescent protein (BFP) were imaged at DIV2 (Fig 2D). While KIF5B-MDC-GFP-FRB predominantly targets cargo into the longest neurite, KIF1C-MDC-GFP-FRB and KIF21A-MDC-GFP-FRB drive transport toward all neurites (Fig 2D). Quantification revealed that KIF1C and KIF21A target at least two neurites in ≥ 90% of the analyzed cells (Fig 2E). In the majority of the KIF1C- and KIF21A-expressing neurons, peroxisomes accumulate in all neurites (Fig 2F). Together, these findings suggest that KIF1 members of the kinesin-3 and KIF21 members of the kinesin-4 subfamily drive non-polarized cargo transport in both developing and differentiated neurons.

DCLK1 is required for KIF1-mediated cargo transport into dendrites

Although we found no kinesin to selectively drive dendritic transport, our data showed that some KIF1 and KIF21 family members were able to target dendrites. These results suggest that dendrite specific cues may exist that facilitate kinesin-dependent cargo distribution in dendrites. Several classical MAPs and other microtubule-binding proteins are restricted to a specific neuronal compartment, and there are several lines of evidence suggesting that kinesin activity is controlled at the level of the microtubule-motor interface (Atherton *et al*, 2013; Franker & Hoogenraad, 2013). An important challenge is thus to identify microtubule-binding proteins that contribute to the dendritic targeting of KIF1 and KIF21 members. In cultured neurons at DIV14, we first determined the distribution of various MAPs that were previously reported to be present in dendrites. MAP1A and MAP1B were present in axons and dendrites at roughly equal levels, while MAP2 and DCLK1 were preferentially concentrated in the somatodendrite region (Fig 3A). Consistent with previous studies (Huber & Matus, 1984; Shin *et al*, 2013), the quantification of the relative ratio of fluorescent intensity in dendrites and axons revealed that MAP2 and DCLK1 are highly enriched in the dendrites (Fig 3B).

We next determined whether these MAPs are involved in KIF1-dependent cargo transport. We used MAP1A, MAP1B, and MAP2 shRNAs based on the previously published sequences to perform knockdown experiments in neurons (Szebenyi *et al*, 2005; Kapitein *et al*, 2011; Tortosa *et al*, 2013) in combination with the KIF1C-inducible cargo trafficking assay. Three shRNA sequences were designed against DCLK1, and each reduced protein levels by ~80% as revealed from both immunostaining and Western blot analysis (Fig 3C–F), indicating an effective knockdown for all DCLK1-shRNA constructs. Depletion of DCLK1 did not affect DCLK2 protein levels (Fig 3E), suggesting specificity of the DCLK1 knockdown. We next analyzed the axon and dendritic trafficking of KIF1C-bound peroxisomes in control and MAP-depleted neurons (Fig 3G and H). In control neurons, ~85% of the cells displayed both axonal and dendritic targeting of KIF1C. While MAP1B and MAP2 depletion did not and MAP1A only mildly affect the distribution of KIF1C-transported cargoes (80–90% and 60% of cells with axon/dendrite targeting, respectively), DCLK1 knockdown markedly reduced the

Figure 2. Kinesin family members display distinct targeting preferences in neurons.

A Representative maximum intensity projections of peroxisome distribution before and after rapalog addition in DIV14 hippocampal neurons expressing PEX-mRFP-FKBP, KIF1C-MDC-FRB, KIF21A-MDC-FRB or KIF5B-MDC-FRB. The morphology of transfected cells is visualized using a BFP fill. Axons are marked with a blue line. Arrows mark peroxisome targeting to dendrites (gray) and axon (blue) 30 min after rapalog addition. Scale bar, 20 μm.

B Plots representing intensity time traces of dendrites and axons before and after rapalog addition for KIF1C-MDC-FRB (n = 6 neurons), KIF21A-MDC-FRB (n = 4) and KIF5B-MDC-FRB (n = 8). Traces were normalized to the average intensity before rapalog addition, and to the background. Error bars indicate SEM.

C Quantitative representation of percentage of DIV14 neurons transfected as in (A) with constructs shown in Fig 1A, in which peroxisomes after the addition of rapalog redistributed to either axons ("a", blue bars) or to axons and at least 2 dendrites ("a + d", red bars). Kinesins were considered "dendrite targeting" if dendrites were targeted in ≥ 50% of cells and are highlighted in red. Kinesin constructs are transfected as indicated; the number of analyzed cells is summarized in Appendix Table S1.

D Representative maximum intensity projections of peroxisome distribution before and after rapalog addition in DIV2 hippocampal neurons transfected as in (A). Scale bar, 20 μm.

E Percentage of DIV2 neurons transfected with KIF1C-MDC-FRB (n = 9 neurons), KIF21A-MDC-FRB (n = 14) and KIF5B-MDC-FRB (n = 14) in which peroxisomes redistributed into at least 2 neurites after the addition of rapalog. Error bars indicate SEM.

F Percentage of neurites of DIV2 neurons transfected as in (E) targeted with peroxisomes after the addition of rapalog. Error bars indicate SEM.

number of cells with axon/dendritic targeting to ~25% (Fig 3H). Instead, in 60% of DCLK1-depleted neurons displayed, KIF1C now selectively targeted the axon (Fig 3G and H). At the same time, DCLK1 knockdown does not affect KIF21 and KIF5 targeting (Fig 3H). These results suggest that DCLK1 is required for KIF1-mediated cargo transport into dendrites.

KIF1 proteins drive dense-core vesicle transport in neurons and are critical for dendrite morphology

We next determined whether DCLK1 is required for the endogenous KIF1 cargo transport. It has been suggested that KIF1 family proteins mediate dense-core vesicle (DCV) trafficking (Zahn *et al*, 2004;

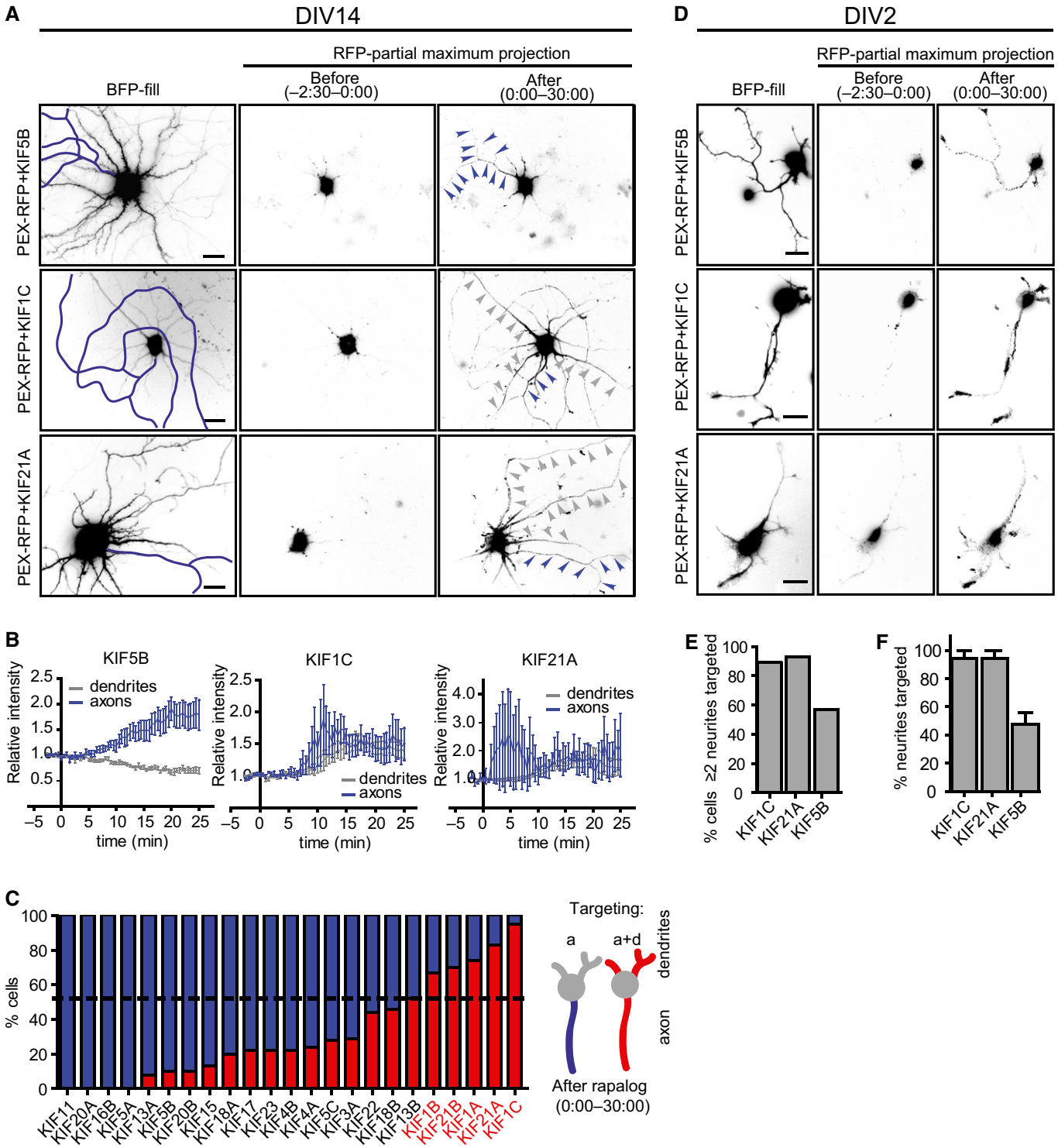

Figure 2.

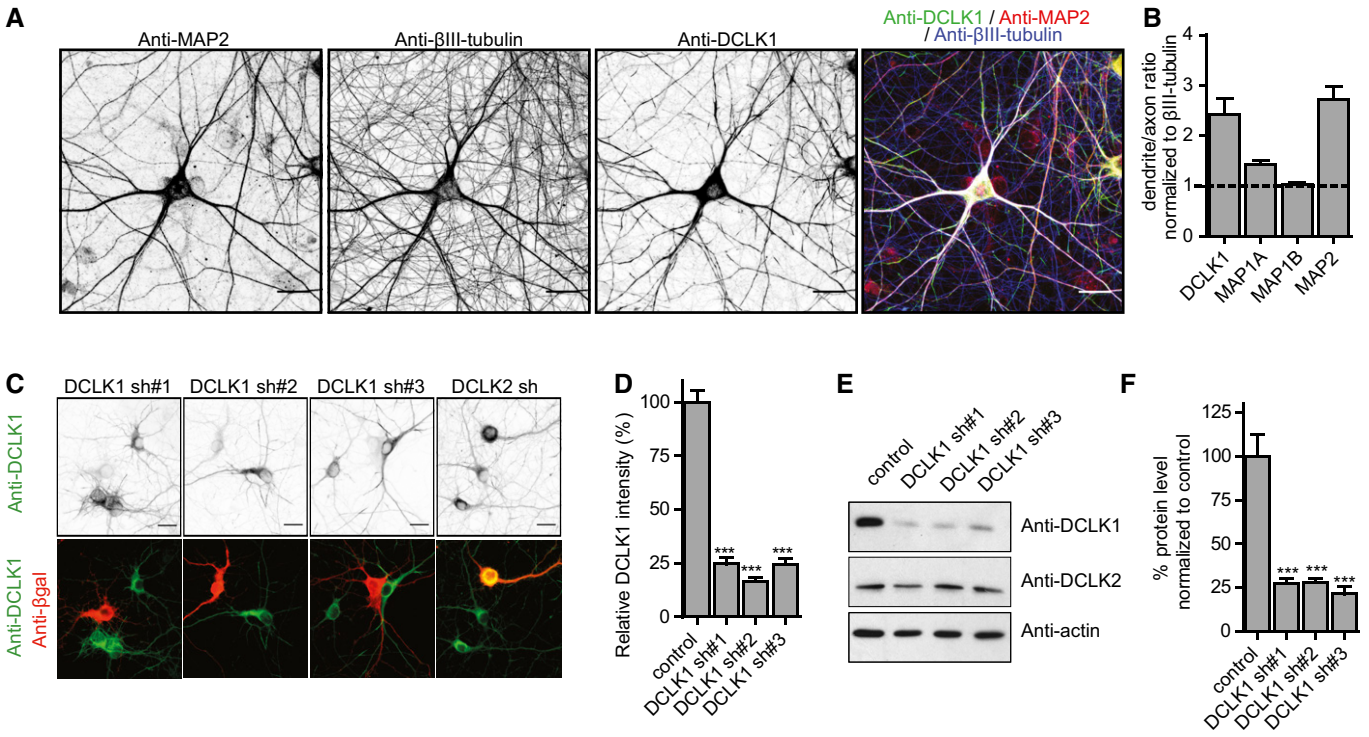

Figure 3. DCLK1 regulates KIF1-mediated transport into the dendrites.

A Representative confocal images of a hippocampal neuron (DIV14) immunostained for MAP2, β-III-tubulin and DCLK1. Scale bar, 20 μm.

B Quantification of the average ratio of DCLK1, MAP1A, MAP1B and MAP2 to total tubulin immunofluorescence intensities in dendrites compared to axons. Six to nine cells were analyzed per condition. Error bars indicate SEM.

C Representative images of DIV10 hippocampal neurons transfected for 4 days with plasmids encoding β-gal for visualizing the transfected cells and three different DCLK1 shRNAs or DCLK2 shRNA and immunostained for β-gal (red) and DCLK1 (green). Scale bar, 20 μm.

D Quantitative analysis of normalized average intensity of DCLK1 in regions of interest of DIV10 neurons transfected with DCLK1 sh#1 (n = 16 neurons), DCLK1 sh#2 (n = 16) and DCLK1 sh#3 (n = 18). Non-transfected cells were taken as a control (n = 48). N = 2. Error bars indicate SEM; ***$P < 0.001$ (one-way ANOVA followed by a Tukey's multiple comparison test).

E Example of Western blot analysis of protein extracts of DIV4 cortical neurons electroporated on DIV0 with pSUPER (control) or pSUPER encoding one of three DCLK1 shRNAs. Levels of actin were used as a loading control.

F Quantification of protein levels of DCLK1 of samples represented in (E). N = 3, error bars indicate SEM, ***$P < 0.001$ (one-way ANOVA followed by a Tukey's multiple comparison test).

G Representative maximum projections of peroxisome distribution in DIV14 neurons transfected with PEX-mRFP-FKBP, KIF1C (MDC)-FRB and the indicated shRNA before and 30 min after rapalog addition. BFP fill was co-transected to visualize the morphology of transfected neuron. Axons are marked with a blue line. Arrows mark dendrite (gray) and axon (blue) targeting of peroxisomes after rapalog addition. Scale bar, 20 μm.

H Quantitative representation of the percentage of DIV14 neurons transfected with PEX-RFP together with either KIF1C, KIF21A or KIF5B and an indicated shRNA, in which after the addition of rapalog peroxisomes redistributed to axons ("a", blue bars), to both axons and dendrites ("a + d", red bars) or did not redistribute into any neuronal compartment ("nt", no targeting, gray bars). 19–44 neurons were analyzed per condition; N = 2.

Barkus *et al*, 2008; Lo *et al*, 2011). Indeed, KIF1A-GFP labeled both motile and static DCVs, as marked by fluorescently tagged neuropeptide Y (NPY) (Fig 4A–C, see also Movie EV3). NPY-mCherry-positive DCVs were transported into both axons and dendrites and moved with an average velocity (1.4 ± 0.9 μm/s) and run length (3.74 ± 3 μm) comparable to previous reports (Lochner *et al*, 2008). The NPY labeled DCVs also contained the secretory proteins brain-derived neurotrophic factor (BDNF) (Fig 4D and E) but did not coincide with the dendritic membrane protein Transferrin Receptor (TfR) (Fig 4F and G). In addition, the average velocity and run length of DCVs and TfR vesicles are markedly different (Fig 4H and I), suggesting that these two populations of vesicles are transported by different motors.

We next determined whether KIF1 is required for DCV cargo transport into dendrites. We generated KIF1A, KIF1B, and KIF1C shRNAs (collectively named KIF1 shRNAs) and performed knockdown experiments in combination with live-cell imaging of NPY-GFP. To specifically visualize NPY-GFP entries into dendrite, the proximal dendrite was first photobleached and directly after imaged with fast acquisition (Fig 4J). Kymographs were used to quantify the number of NPY-GFP entries and their dynamics (Fig 4K). In KIF1-depleted neurons, the number of NPY-GFP entries into the dendrite is strongly reduced compared to control cells and KIF21 knockdown neurons (Fig 4L). Knockdown of KIF1A or KIF1C strongly decreased the number of dendritic NPY-GFP vesicles, while depletion of KIF1B did not affect NPY-GFP trafficking (Fig 4L). The dendrite selective transport of Transferrin Receptor (TfR) vesicles was not altered in KIF1-depleted neurons (Fig 4M and N). These data indicate that KIF1A and KIF1C are required to drive DCVs into dendrites.

Previous studies showed that DCVs causes dendritic growth by the release of peptide neuromodulators (Horch & Katz, 2002; Lazo *et al*, 2013). Recent results suggest that DCLK1 is also involved in dendrite development (Shin *et al*, 2013). Indeed, we found that depletion of endogenous DCLK1 in DIV10 neurons affected the complexity of the dendritic branching and total dendritic length (Fig 4O–Q). This phenotype is very similar to the reduced dendritic complexity observed in KIF1 deficient neurons (Fig 4O–Q). Thus, together these data suggest that the DCLK1/KIF1-dependent trafficking of DCVs is required for proper dendrite morphology.

DCLK1 regulates dense-core vesicle transport into dendrites

To further determine the precise role of DCLK1 in DCV trafficking, we depleted endogenous DCLK1 in DIV14 hippocampal neurons and analyzed the trafficking of NPY-GFP into dendrites. The number of dendritic NPY-GFP entries is strongly reduced in DCLK1 knockdown neurons compared to control cells (Fig 5B and C, see also Movie EV4). The impaired DCV trafficking phenotype was partly rescued by expression of an shRNA-resistant form of full-length DCLK1 (Fig 5B and C). TfR receptor vesicle trafficking was not altered in DCLK1-depleted neurons (Fig 5D and E). These results indicate that DCLK1 is required to drive DCVs into dendrites.

DCLK1 contains two C-terminal "doublecortin" microtubule-binding (MTB) domains and an N-terminal kinase (KD) domain (KD) (Fig 5A). To determine which DCLK1 domain is required for DCLK1 function, we cotransfected neurons with DCLK1 shRNA and C- or N-terminal deletion mutants: DCLK1(ΔKD)-GFP (RNAi-resistant DCLK1 without a kinase domain) and DCLK1(ΔMTB)-GFP (RNAi-resistant DCLK1 without the microtubule-binding domains). In DCLK1-depleted neurons, expression of DCLK1(ΔKD)-GFP, and not DCLK1(ΔMTB)-GFP, rescued the dendritic DCV trafficking defects (Fig 5B and C). In addition, DCLK1(MAP2)-GFP (RNAi-resistant DCLK1 where the MTB of DCLK1 is replaced with the MTB of MAP2) did not rescue the DCLK1 phenotype (Fig 5B and C). Together, these results suggest a critical role for the DCLK1 MT-binding domains in DCV trafficking.

Figure 4. KIF1 drives transport of dense-core vesicles in dendrites and is essential for proper dendritic morphology.

A–G Representative frame (A, D) and a kymograph (B, F) of a simultaneous two-color movie of a hippocampal neuron expressing NPY-mCherry and either KIF1A-GFP (A, B), BDNF-GFP (D), or TfR-GFP (F). Scale bars, 20 μm (A, D) or 5 μm (B, F). (C) Quantification of vesicle colocalization in cells described in (A, B). The quantification indicates the % of KIF1A vesicles that are NPY positive: left bar quantified from images of fixed cells presented in (A) and right bar quantified from kymographs as presented in (B) (only moving fraction). (E) Quantification of vesicle colocalization in cells described in (D): The left bar indicates the % of NPY vesicles that are BDNF positive, the right bar indicates the % of BDNF vesicles that are NPY positive. (G) Quantification of vesicle colocalization in cells described in (F). The left bar indicates the % of NPY vesicles that are TfR positive, the right bar indicates the % of TfR that are NPY positive. Error bars indicate SEM.

H, I Quantification of run lengths (H) and velocities (I) of vesicles in dendrites of hippocampal neurons transfected at DIV10–14 for 4 days with either NPY-GFP (n = 924 movements), TfR-GFP (n = 286) or KIF1A-GFP (n = 174) together with a morphology marker BFP. N = 2. Error bars indicate SEM; ***$P < 0.001$ (one-way ANOVA followed by a Tukey's multiple comparison test).

J Scheme of live-cell imaging after photobleaching to visualize the motility of dense-core vesicles labeled with NPY-GFP (H, I, K, L) or TfR-positive recycling endosomes (H, I, M, N) in proximal dendrites of hippocampal neurons (DIV14).

K Representative kymographs of NPY-GFP-labeled dense-core vesicle motility in primary dendrites of transfected neurons. DIV10–14 hippocampal neurons were cotransfected for 4 days with plasmids encoding NPY-GFP, BFP fill and either KIF21 shRNA mix (n = 30), KIF1 shRNA mix (n = 31), KIF1A shRNA (n = 19), KIF1B shRNA (n = 19) or KIF1C shRNA (n = 11). pSUPER was used as a control (n = 15). Scale bar, 5 μm.

L Quantification of the average number of dense-core vesicle entries into the primary dendrite of neurons from (K) in 100 s after photobleaching. N = 2–3. Error bars indicate SEM; ***$P < 0.001$ (one-way ANOVA followed by a Tukey's multiple comparison test).

M Representative kymographs of TfR-GFP-labeled recycling endosome motility in primary dendrites. DIV10–14 hippocampal neurons were cotransfected with TfR-GFP together with a BFP fill and a KIF1 shRNA mix (n = 11). pSUPER was used as a control (n = 20). Scale bar, 5 μm.

N Quantification of the average number of recycling endosome entries into the primary dendrite of neurons from (M) in 50 s. N = 2. Error bars indicate SEM. ns, not significant (Mann–Whitney test).

O Representative images of hippocampal neurons (DIV4) cotransfected with an empty pSUPER (control) or pSUPER encoding an indicated shRNA together with a GFP fill fixed at DIV8 and immunostained for MAP2 and sodium channels (AIS). Scale bar, 50 μm.

P Sholl analysis of cells described in (O). Error bars indicate SEM; *$P < 0.05$, **$P < 0.01$, and ***$P < 0.001$ (two-way ANOVA test followed by Bonferroni's *post hoc* test).

Q Analysis of the total dendritic length of cells described in (O). Error bars indicate SEM; *$P < 0.05$, **$P < 0.01$ and ***$P < 0.001$ (one-way ANOVA followed by a Tukey's multiple comparison test). 21–24 neurons (n) were analyzed per condition; N = 2.

Published online: January 12, 2016

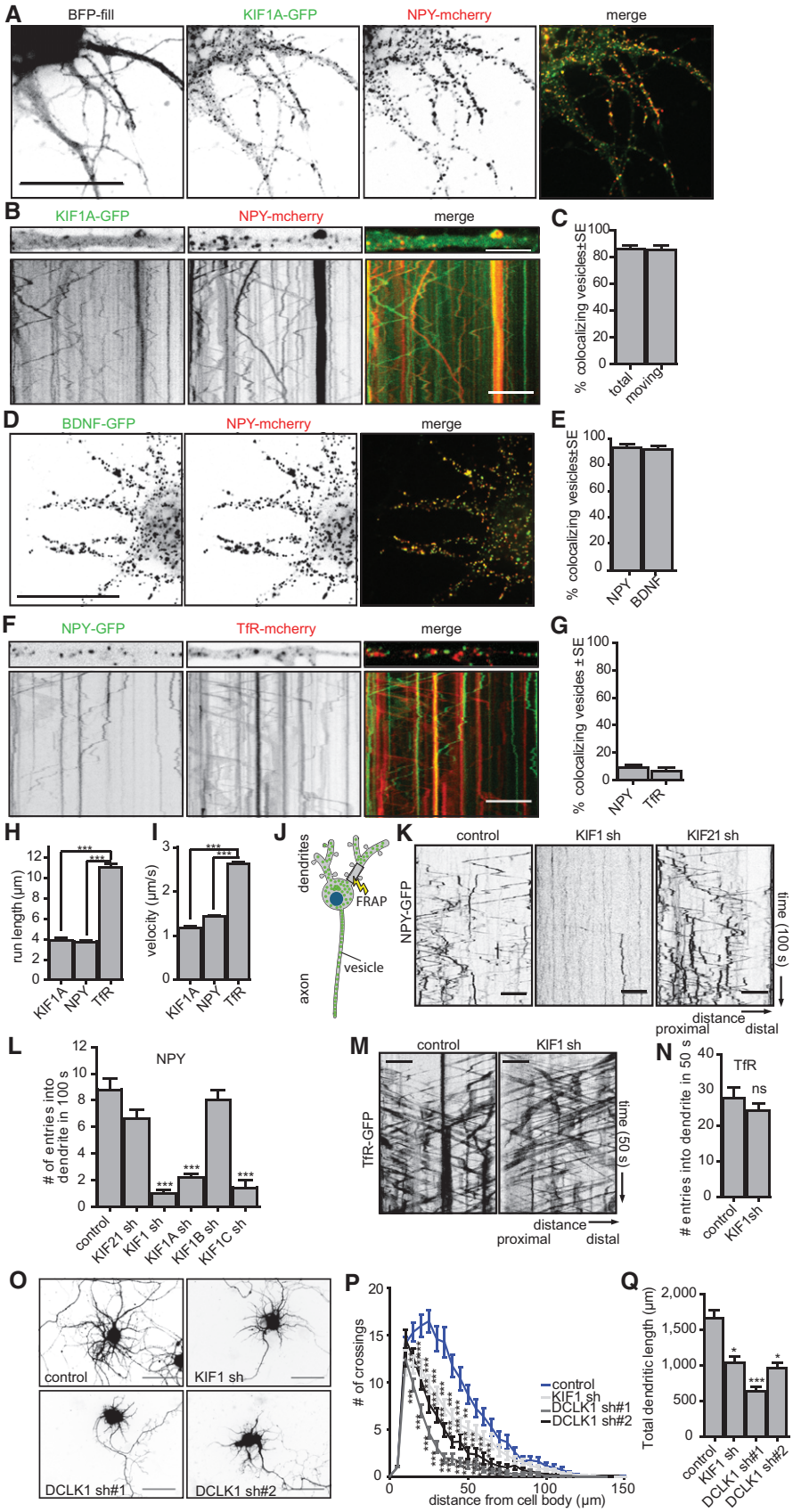

Figure 4.

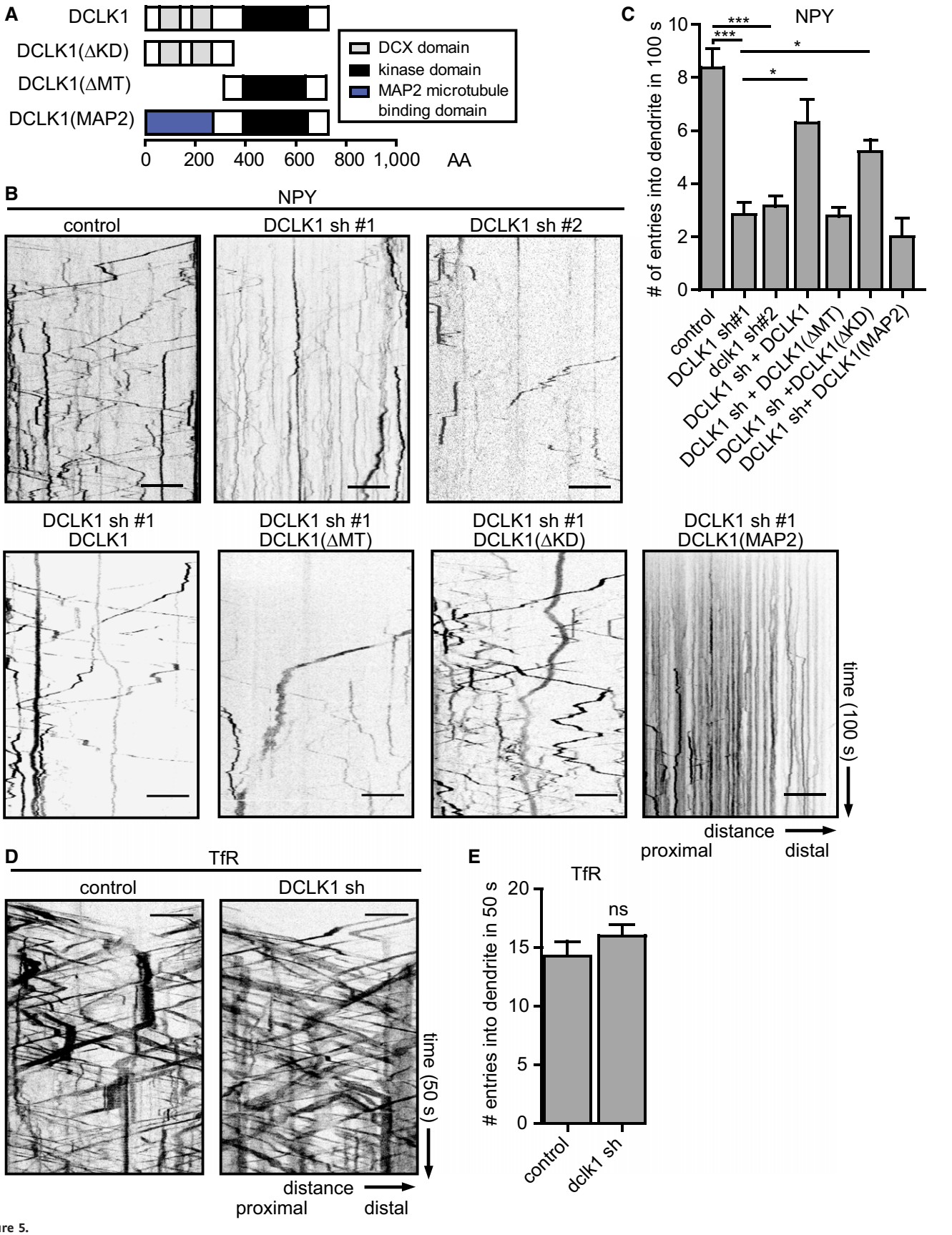

Figure 5.

Figure 5. DCLK1 regulates dense-core vesicle entry into the dendrite.

A Scheme of DCLK1 truncation constructs.

B Representative kymographs of dense-core vesicle motility in proximal dendrites of transfected neurons. DIV10–14 hippocampal neurons were co-transfected for 4 days with NPY-GFP and pSUPER (control) or pSUPER encoding DCLK1 shRNA in the absence or presence of DCLK1 truncation constructs and dense-core vesicle motility in dendrites was recorded during live-cell imaging. Scale bar, 5 μm.

C Quantification of the average number of dense-core vesicle entries into dendrites of neurons transfected as in (B) during 100 s of the live recording after photobleaching. 10–32 cells were analyzed per condition. Error bars indicate SEM; ***$P < 0.001$ (Kruskal–Wallis test followed by *post hoc* Dunn's test). $N = 2$. *$P < 0.05$.

D, E DIV10–14 hippocampal neurons were co-transfected for 4 days with either pSUPER (control, $n = 20$ neurons) or DCLK1 shRNA together with TfR-GFP ($n = 16$). (D) Representative kymographs of recycling endosome motility in dendrites. Scale bar, 5 μm. (E) Quantification of the average number of recycling endosome entries into dendrites during 50 s of the live recording after photobleaching. Error bars indicate SEM; ns, not significant (Mann–Whitney test). $N = 2$.

DCLK1 preferentially associates with dynamic microtubules

DCLK1 controls DCV transport into dendrites, but little is known about the expression and distribution of DCLK1 in differentiated neurons. In contrast to transient DCX expression in newly generated and immature neurons (Francis *et al*, 1999; Gleeson *et al*, 1999a), DCLK1 is present throughout hippocampal development and maintained in more mature neurons (Fig 6A). Immunocytochemistry of mature hippocampal neurons at DIV14 with DCLK1 antibodies revealed a marked somatodendritic staining (Fig 3A and B). High-resolution images showed that DCLK1 strongly colocalizes with microtubules in dendrites (Fig 6B). Due to the high microtubule density in dendrites, we cannot unambiguously separate individual microtubules. We moved to COS-7 cells where the microtubule array is rather sparse and individual microtubules can be distinguished. In COS-7 cells, DCLK1-GFP is excluded from the stable (detyrosinated) microtubule population, labels dynamic microtubules along their length and accumulates in long stretches near the microtubule ends at the cell periphery (Fig 6C). Similar results were obtained by expression of DCLK1(ΔKD)-GFP in COS-7 cells (Fig 6D). The ability of DCLK1 to associate with dynamic microtubules was further confirmed by simultaneous dual-color live imaging of DCLK1-GFP and TagRFP-EB3: EB3 labels the growing microtubule plus-end of DCLK1-labeled dynamic microtubules (Fig 6E). These data are consistent with recent *in vitro* studies, where DCX was shown to recognize a subset of microtubules and is able to associate with growing microtubule ends (Bechstedt & Brouhard, 2012).

Proper microtubule polarity in DCLK1-depleted dendrites

How does DCLK1 control KIF1 cargo transport into dendrites? DCLK1 interacts with microtubules and may indirectly affect DCV trafficking by changing microtubule polarity in dendrites. We first tested for stable and dynamic microtubule markers. Western blot analysis revealed that DCLK1 depletion does not affect the levels of total, acetylated and tyrosinated tubulin (Fig 7A). Neurons expressing DCLK1 shRNA and stained for EB3 as a marker of dynamic microtubules (Jaworski *et al*, 2009) showed that the characteristic comet-like microtubule plus-end pattern was slightly increased in the soma and dendrites (Fig 7B–D), suggesting that DCLK1 may have a role in regulating microtubule dynamics. We next tested whether DCLK1 controls the organization of mixed microtubules in dendrites. Control neurons show an anti-parallel microtubule organization with GFP-MT+TIP comets growing toward the soma (retrograde, plus-end-in) and dendritic tips (anterograde, plus-end-out) (Fig 7E). In DCLK1-depleted neurons, the GFP-MT+TIP comets grow in opposite directions similar to control cells (Fig 7E and F). To elucidate in more detail the orientations of dynamic and stable microtubules, we use live-cell imaging of GFP-MT+TIPs in combination with laser-based microsurgery (Yau *et al*, 2014). Analyzing the growth direction of GFP-MT+TIP comets after laser severing revealed that the mixed microtubule orientations in dendrites are of roughly equal ratio in both control and DCLK1 knockdown neurons (Fig 7G and H). Together these data suggest that DCLK1 is not critically involved in microtubule organization in dendrites.

The N-terminal region of DCLK1 associates with the motor domain of KIF1

Previous studies have shown that DCX and KIF1A directly interact and form a ternary complex with microtubules (Liu *et al*, 2012). Here we tested whether DCLK1 can associate with KIF1 family members (Fig 7I–K). Constructs encoding biotinylated and GFP-tagged full-length DCLK1 (DCLK1-GFP-bio) and HA-tagged truncated KIF1 (KIF1A-MDC and KIF1C-MDC) were transiently expressed in HEK293 together with the protein biotin ligase BirA. Biotinylated DCLK1 proteins were isolated with streptavidin beads and further analyzed by Western blotting. DCLK1 specifically pulled down truncated KIF1A and KIF1C (Fig 7I), indicating that DCLK1 associates with the motor domain/coiled-coil region of KIF1 family members. Deletion of the KIF1A coiled-coil region showed that DCLK1 is able to associate with a single motor domain (Fig 7J). Full-length KIF1A was used as a positive control. By expressing the N-terminal domain (DCLK1(ΔKD)-GFP) and C-terminal domain (DCLK1(ΔMTB)-GFP) regions, we mapped the KIF1-binding region of DCLK1 (Fig 7K). While the C-terminal kinase domain was not able to interact with KIF1A, the microtubule-binding region bound to KIF1A (Fig 7K). Together, these data indicate that the N-terminal region of DCLK1 associates with the motor domain of KIF1 and suggest that DCLK1 at the microtubule surface controls specific kinesin-mediated cargo transport into dendrites.

Discussion

In this study, we demonstrate that KIF1 and KIF21 family members can drive cargo transport into both the axon and dendrites. The dendrite targeting of KIF1 is regulated by the microtubule-binding protein DCLK1. DCLK1 is a close homologue of doublecortin (DCX), which is mutated in X-linked lissencephaly and double-cortex syndrome (Gleeson *et al*, 1999b). The N-terminal domain of DCLK1 is almost identical to DCX and associates with microtubules (Kim *et al*, 2003). In contrast to DCX, DCLK1 remains expressed in developing and mature neurons. We found that DCLK1 labels dendritic

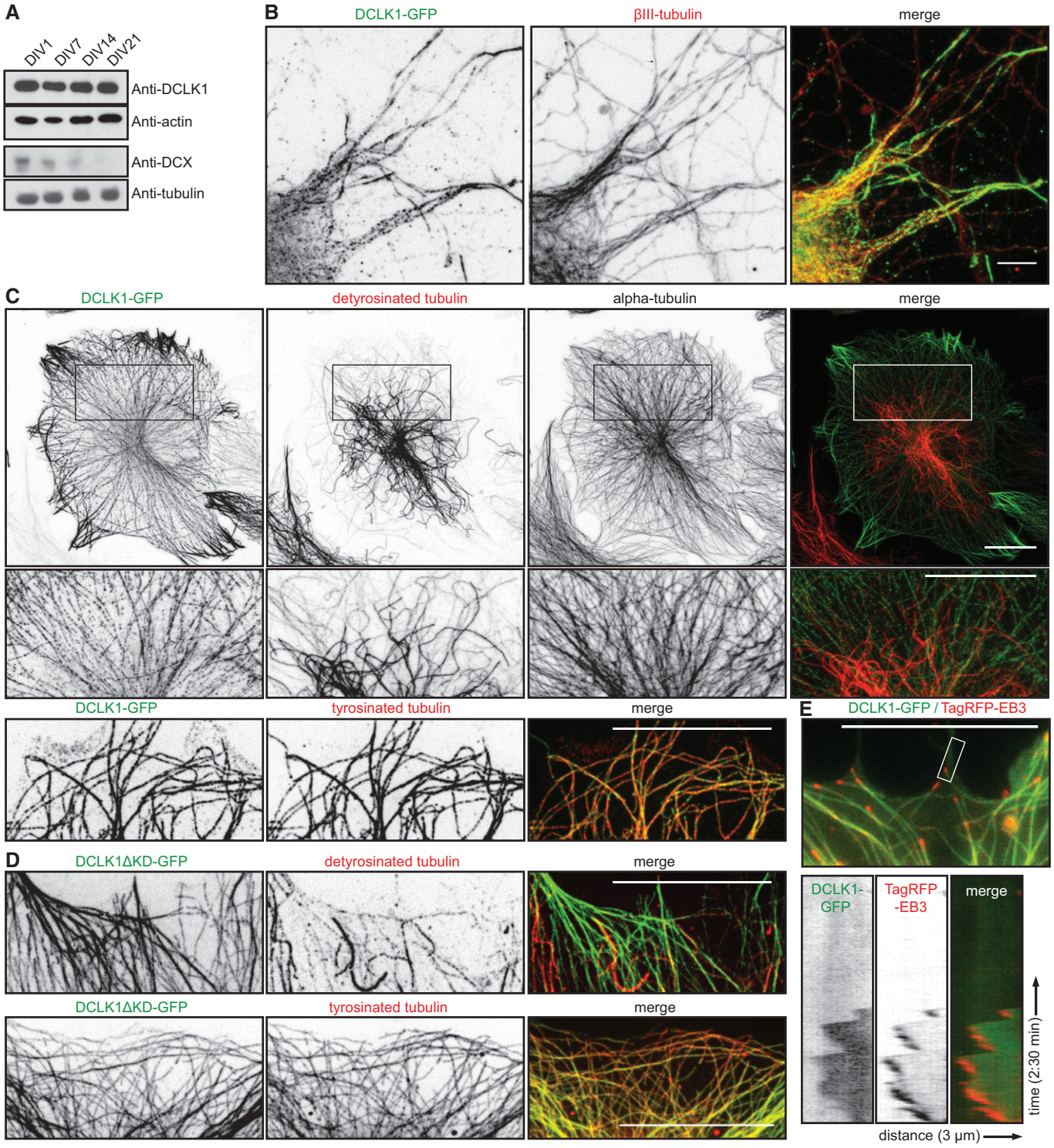

Figure 6. DCLK1 preferentially binds to a subset of microtubules.

A Example of Western blot analysis of DCLK1 and DCX levels in protein extracts obtained from DIV1, DIV7, DIV14, and DIV21 hippocampal neurons. Levels of tubulin were used as a loading control.

B Representative image of a hippocampal neuron (DIV14) immunostained for DCLK1 and β-III-tubulin. Scale bar, 20 μm.

C, D Representative image of a COS-7 cell transfected with DCLK1-GFP (C) or DCLK1(ΔKD)-GFP (D) and stained for detyrosinated, tyrosinated or α-tubulin. Scale bar, 20 μm.

E Representative image of a COS-7 cell transfected with DCLK1-GFP and TagRFP-EB3 and recorded during live-cell imaging. Representative kymograph was drawn (over a region marked with white boxes) showing that DCLK1-GFP colocalizes with EB3-TagRFP-T. Scale bar, 20 μm.

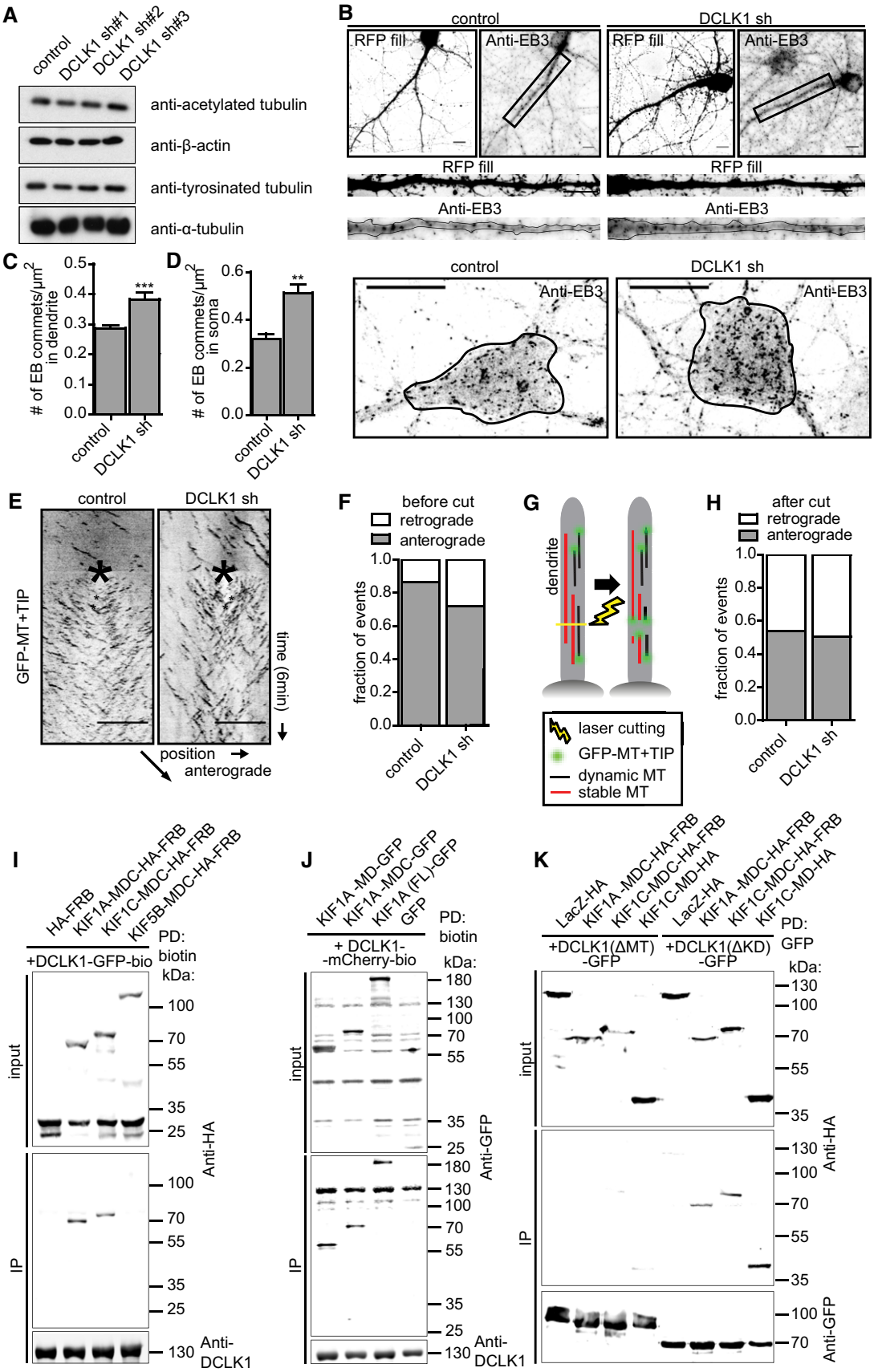
A
control
DCLK1 sh#1
DCLK1 sh#2
DCLK1 sh#3
anti-acetylated tubulin
anti-β-actin
anti-tyrosinated tubulin
anti-α-tubulin
B
control
DCLK1 sh
RFP fill
Anti-EB3
C
# of EB comets/μm2 in dendrite
D
# of EB comets/μm2 in soma
E
GFP-MT+TIP
time (6min)
position
anterograde
F
before cut
retrograde
anterograde
fraction of events
G
dendrite
laser cutting
GFP-MT+TIP
dynamic MT
stable MT
H
after cut
I
HA-FRB
KIF1A-MDC-HA-FRB
KIF1C-MDC-HA-FRB
KIF5B-MDC-HA-FRB
+DCLK1-GFP-bio
PD: biotin
kDa:
input
IP
Anti-HA
Anti-DCLK1
J
KIF1A-MD-GFP
KIF1A-MDC-GFP
KIF1A (FL)-GFP
GFP
+ DCLK1-mCherry-bio
Anti-GFP
K
LacZ-HA
KIF1A-MDC-HA-FRB
KIF1C-MDC-HA-FRB
KIF1C-MD-HA
+DCLK1(ΔMT)-GFP
+DCLK1(ΔKD)-GFP
PD: GFP

Figure 7.

Figure 7. DCLK1 associates with KIF1 and does not affect microtubule polarity in dendrites.

A Extracts of DIV7 hippocampal neurons electroporated with pSUPER control or with three different DCLK1 shRNAs at DIV0. Samples were analyzed by Western blot with the indicated antibodies.

B Representative images of a hippocampal cell transfected at DIV10 with RFP (to visualize transfected cells), pSUPER (control) or DCLK1 shRNA, fixed at DIV14 and stained for EB3. Black lines indicate the neuronal soma outline. Scale bars, 10 μm.

C, D Quantification of the number of EB3 comets in the dendrite (C) and in the soma (D). 25–26 neurons were analyzed per condition, $N = 2$. Error bars indicate SEM, $^{***}P < 0.001$, $^{**}P < 0.01$ (unpaired *t*-test).

E–H Hippocampal neurons were co-transfected with MACF18-GFP and pSUPER (control) or DCLK1 shRNA and the dynamics of microtubules in dendrites was traced using life-cell microscopy. (F) Representative kymographs of dynamic microtubules' end growth in dendrites with and without photoablation. Scale bar, 10 μm. (G, I) Quantification of the fraction of MACF18 events moving retrogradely and anterogradely in a dendrite before (G) and after (I) photoablation. Eighteen neurons were analyzed per condition; $N = 2$. (H) Scheme of live-cell imaging after photoablation.

I, J Biotin pull-downs (PD) from extracts of HEK293 cells transfected with biotin-tagged DCLK1 and (I) KIF1A-MDC-HA-FRB, KIF1C-MDC-HA-FRB, KIF5B-MDC-HA-FRB constructs and probed for HA/DCLK1, or (J) different GFP-tagged KIF1A truncation constructs and probed for GFP/DCLK1. The ratio input/pellet is 2% for all pull-down experiments.

K GFP pull-down from extracts of HEK293 cells transfected with DCLK1 fragments and KIF1A-MDC-HA-FRB, KIF1C-MDC-HA-FRB and KIF1C-MD-HA and probed for HA/GFP. LacZ-HA was used as a negative control.

microtubules and is required for KIF1-dependent dense-core vesicle (DCV) trafficking and dendrite development. The results suggest a model in which DCLK1 at the microtubule surface represents a regulatory signal for enhancing KIF1 motor activity in dendrites.

Polarized cargo transport is controlled at the microtubule-motor interface

Probing polarized transport of endogenous transport carriers is challenging because cargos typically have different types of motors attached, precluding direct determination of the active motor type that is driving polarized transport. In this study, we used an inducible cargo trafficking assay to test for targeting properties of all 45 known kinesin family members. Here we found that roughly half of the kinesin superfamily members we evaluated are able to translocate cargo in living cells. This does not necessarily mean that other kinesins are not able to transport cargo in living cells. By creating truncated kinesin constructs it is possible that some of the kinesin family members are non-functional due to incorrect protein folding or that they are missing critical components of the native motor complex. Moreover, kinesins identified as "cargo translocators" do not necessarily transport endogenous cargo in living cells. For instance, KIF21A, which is named a "cargo translocator" in our study has been shown to be a suppressor of microtubule growth (van der Vaart *et al*, 2013) while its function in cargo transport is not documented.

Consistent with *in vitro* studies, we found that the kinesin members have different transport characteristics. Even kinesin members within the same subfamily have different transporting properties and targeting preferences suggesting that primary sequence conservations and structural similarities do not necessarily account for similar motor functions. We found that none of the kinesins selectively target dendrites and only five members of the kinesin-3 (KIF1A/B/C) and kinesin-4 (KIF21A/B) families drive transport into both the axon and dendrites. The data are largely consistent with experiments in fixed neurons where the axonal and dendritic accumulations of some of the major kinesin members were quantified (Huang & Banker, 2012). Nevertheless, some motors, such as KIF21A, target the dendrites when bound to cargo. It is also important to note that in this study, we evaluated which kinesins mediate selective transport from the cell body into axons and/or dendrites. Previous data have shown that while most kinesin family members hardly drive transport from the cell body into dendrites, some of them can induce bidirectional motility of cargo that is already present within dendrites (Kapitein *et al*, 2010a). These data indicate that a select team of kinesin and dynein motors establishes the initial cargo sorting from the cell body to the dendrites, whereas other motors can assist in cargo motility once the vesicle is inside dendrites. Moreover, dynein has also been shown to mediate dendrite selective cargo transport over minus-end-out microtubules (Kapitein *et al*, 2010a). It is very likely that dendritic transport selectivity is achieved by cooperative actions of KIF1 and dynein motors. Future studies on polarized cargo transport should investigate the role of different motor combinations.

The use of truncated kinesin constructs in which the cargo-binding domain and most of the tail region is deleted, revealed that the motor domain and first coiled-coil region are sufficient to drive polarized cargo transport in neurons. These results demonstrate that selective cargo trafficking can be controlled at the level of the microtubule-dimeric motor interface. However, additional regulatory mechanisms are likely to be involved. For instance, our results showed that all truncated transporting kinesins are able to drive robust cargo trafficking into the axon, indicating that the regulatory factor for selective cargo sorting at the axon initial segment is absent in this trafficking system. Moreover, it has been clearly demonstrated that some kinesins, such as KIF11 (Eg5) and KIF17 which in our assay are selectively targeting the axon, are present in dendrites (Ferhat *et al*, 1998; Guillaud *et al*, 2003). Thus, it is very likely that additional motors, adaptor proteins, or signaling factors present on endogenous transport carriers provide additional levels of regulation (Ou *et al*, 2010; Farias *et al*, 2012; Watanabe *et al*, 2012; van Spronsen *et al*, 2013a). Indeed, several studies report that additional kinesin-3 regulatory mechanisms exist that involves the interaction of tail domain (Hammond *et al*, 2009). Therefore, mimicking endogenous neuronal cargo transport by recruiting additional regulatory complexes to transport carriers will be a major challenge for future work.

DCLK1 is required for DCV trafficking and dendrite development

Dendritic growth and branching is associated with polarized secretory vesicle trafficking (Horton *et al*, 2005; Ye *et al*, 2007; Quassollo *et al*, 2015). Here we show that neurons lacking DCLK1 or members of the kinesin-3 family (KIF1) fail to develop proper dendrite

morphology. These data are consistent with the dendritic phenotype observed in neocortical pyramidal neurons of mice after *in utero* electroporation of DCLK1 shRNAs (Shin *et al*, 2013). We also found that DCLK1 regulates dense-core vesicle (DCV) transport into dendrites. DCVs are generated at the Golgi and then trafficked before they are secreted at the plasma membrane (Kim *et al*, 2006). Previous studies showed that DCVs are essential for proper neuronal development by the release of their peptide neuromodulators (Horch & Katz, 2002; de Wit *et al*, 2006; Schlager *et al*, 2010; Lazo *et al*, 2013). Our data suggest that the DCLK1 controls dendritic outgrowth and branching by controlling KIF1-dependent DCV trafficking. It is tempting to speculate that the dendritic DCLK1 depletion phenotype is caused by DCV mistargeting and the subsequent reduction of secretory events in developing dendrites. This is consistent with previous observations that increased retrograde transport of DCVs and accumulation of NPY, Sema3A and BDNF in the cell body reduces dendritic outgrowth (Schlager *et al*, 2010). At early stage of neuronal development, DCVs are coupled to KIF1 and dynein via cargo adaptor protein Bicaudal-D-related protein 1 (BICDR-1) and this motor–adaptor complex is responsible for coordinating bidirectional DCV transport (Schlager *et al*, 2014). This indicates that various molecular mechanisms exist that control DCV trafficking to ensure temporal and spatial regulation of secretion events. Our data suggest that DCLK1 is particularly involved in dendritic targeting of DCVs.

Regulation of KIF1 transport through interactions with DCLK1

How does DCLK1 control KIF1-dependent cargo transport into dendrites? DCLK1 interacts with microtubules and may provide local control of KIF1-mediated vesicle trafficking into dendrites. Several lines of evidence support this model. First, we found that DCLK1 is present in developing and mature neurons and preferentially associates with a specific subset of microtubules. These data are consistent with a recent study, where pan-DCLK antibodies predominately stained the somatodendritic compartment of cultured hippocampal neurons (Shin *et al*, 2013). We also found that DCLK1 does not affect microtubule polarity in dendrites, which suggests that the impairments in dendrite targeting caused by DCLK1 knockdown are not a result of a change in microtubule orientation. Second, we show that the microtubule-binding domain (MTBD) of DCLK1 associates with the KIF1A and KIF1C motor domain. The results are similar to the reported binding regions of DCX and KIF1A (Liu *et al*, 2012). Testing the functional effect of the purified MTBD on microtubule binding and KIF1 motility will be required to fully explore our model. Third, we found that DCLK1 is required for KIF1-mediated cargo transport into dendrites. Previous studies showed that lack of DCX decreases the run length of KIF1A motors and its associated cargo in axons of young neurons (Liu *et al*, 2012). The observed decrease in run length correlated with a decreased affinity of ADP-bound KIF1A motor domain to microtubules in the absence of DCX. It has been hypothesized that DCX reduces KIF1 detachment from the microtubules after completion of its ATPase cycle and therefore promotes cargo transport. Combined with our neuronal trafficking data, these results suggest that DCX family members promote KIF1 motor function. We propose that KIF1 motor activity may be locally enhanced in specific neuronal compartments where DCX family proteins are enriched. In our case the preferential association of DCLK1 with dendritic microtubules may provide local control over KIF1 activity into dendrites. In this way, microtubules decorated with DCLK1 promote KIF1-mediated vesicle trafficking into dendrites, and possibly exclude trafficking of cargo carried by other motors. However, upon knockdown of DCLK1 we did not observe dendritic targeting of KIF5 family members. Therefore, DCLK1 is not an excluding factor for—at least—KIF5. This "exclusion" mechanism may however exist for other kinesin family members.

The action of DCX family proteins is distinct from the many other regulatory mechanisms that control kinesin motor activity at the microtubule-motor level (Schlager & Hoogenraad, 2009; Janke & Kneussel, 2010). DCX binds to the pockets between protofilaments at the corners of four αβ-tubulin dimers and stabilizes 13-protofilament microtubules, suggesting that DCX family proteins can somehow dictate or "measure" protofilament number (Fourniol *et al*, 2010; Bechstedt & Brouhard, 2012). In addition to enhancing KIF1 activity by direct binding with DCLK1 at the microtubule surface, DCLK1 may also influence the microtubule lattice structure and indirectly facilitate KIF1 motor domain binding. Identifying the unique dendritic microtubule features that promote DCLK1 binding is a key challenge for future work.

Highly compartmentalized neurons need efficient regulation machinery to ensure proper delivery of cargo to appropriate destination. Understanding the molecular mechanism of transport is of critical importance since numerous motors and their regulators have been implicated in a wide array of neurodegenerative disorders such as Huntington's disease, amyotrophic lateral sclerosis and multiple sclerosis (Franker & Hoogenraad, 2013; Millecamps & Julien, 2013). Growing evidence suggests that microtubule-associated proteins may regulate motor protein transport. Here we show that DCLK1 promotes KIF1-mediated cargo trafficking into dendrites. Our study demonstrates that microtubule-binding proteins can provide local signals for specific kinesin motors to drive polarized cargo transport in neurons. In analogy to the previously coined "tubulin code" (Janke, 2014), the specific distribution of microtubule-associated proteins may form a "MAP code", in which microtubule-binding proteins regulate the activity of specific kinesin family members (Liu *et al*, 2012).

Materials and Methods

Ethics statement

All animal experiments were performed in compliance with the guidelines for the welfare of experimental animals issued by the Government of The Netherlands. All animal experiments were approved by the Animal Ethical Review Committee (DEC) of Utrecht University.

Antibodies and reagents

The following antibodies were used in this study: rabbit anti-DCLK1 (Abcam, cat#ab31704), rabbit anti-DCLK2 (Abcam, cat#ab106639), chicken anti-MAP2 (Abcam, cat#ab5392), goat anti-MAP1A (Santa Cruz Biotechnology, cat#sc8969), goat anti-MAP1B (Santa Cruz Biotechnology, cat#sc8970), goat anti-DCX (Santa Cruz Biotechnology, cat#sc8066), mouse anti-β-III-tubulin (Sigma-Aldrich, cat#082M4845), mouse anti-α-tubulin (Sigma-Aldrich, cat#T-5168),

rabbit anti-detyrosinated tubulin (Millipore, cat#AB3201), mouse anti-acetylated tubulin (Sigma-Aldrich, cat#T7451), rat anti-tyrosinated tubulin (Abcam, cat#ab6160), and rabbit anti-EB3 (Stepanova *et al*, 2003). For details, see Appendix Supplementary Materials and Methods.

DNA constructs

To generate truncated kinesin (MDC) constructs for the cargo trafficking assay, the first coiled-coil regions were identified in the protein structure of kinesins using COILS prediction software. Next appropriate sequences were inserted into pβactin-GFP-FRB and/or pβactin-HA-FRB vector. The DCLK1 expression constructs were a kind gift from Shigeo Okabe (Shin *et al*, 2013; NM_019978). The following sequences were targeted by shRNAs used in this study: DLCK1 sh#1 (5′-AGGTGGAATGGTATCCAAT-3′; NM_053343.3), DLCK1 sh#2 (5′-GCACGTTAAATCATGGTTG-3′; NM_053343.3), and DLCK1 sh#3 (5′-CTGAGACCCTTAATGTTAC-3′; NM_053343.3). For details, see Appendix Supplementary Materials and Methods.

Primary hippocampal neuron cultures, transfection, and nucleofection

Primary hippocampal and cortical cultures were prepared from embryonic day-18 (E18) rat brains and transfected using Lipofectamine 2000 (Invitrogen) or the Amaxa Rat Neuron Nucleofector kit (Lonza), respectively. For details, see Appendix Supplementary Materials and Methods.

Live-cell imaging and laser-induced severing

Simultaneous dual-color time-lapse live-cell imaging and TIRFM was performed on a Nikon Eclipse TE2000E microscope with Coolsnap and QuantEM cameras (Roper Scientific). Neurons were maintained at 37°C with 5% CO_2 (Tokai Hit). A Teem Photonics 532-nm Q-switched pulsed laser is used for laser-induced severing. The FRAP experiments were performed on a spinning disk microscope system using the ILas2 system (Roper Scientific). For details, see Appendix Supplementary Materials and Methods.

Expanded View for this article is available online.

Acknowledgements
We thank Prof. Shigeo Okabe for sharing DCLK1 constructs. This work was supported by the Netherlands Organization for Scientific Research (NWO-ALW-VIDI, LCK; NWO-ALW-VICI, CCH), the Foundation for Fundamental Research on Matter ((FOM) CCH), which is part of the NWO, the Netherlands Organization for Health Research and Development (ZonMW-TOP, CCH), the European Research Council (ERC) (ERC-starting, LCK; ERC-consolidator, CCH). JL is supported by International PhD Projects Programme of Foundation for Polish Science (studies of nucleic acids and proteins—from basic to applied research) cofinanced by the European Union Regional Development Fund. JJ is supported by Polish National Science Centre Sonata Bis grant (2012/07/E/NZ3/00503) and the Foundation for Polish Science "Mistrz" Professorial Subsidy.

Author contributions
JL designed and performed experiments, analyzed data, and wrote the manuscript; JJ and LCK gave advice throughout the project and edited the manuscript; and CCH designed experiments, coordinated the study, and wrote the manuscript.

Conflict of interest
The authors declare that they have no conflict of interest.

References

Atherton J, Houdusse A, Moores C (2013) MAPping out distribution routes for kinesin couriers. *Biol Cell* 105: 465 – 487

Baas PW, Deitch JS, Black MM, Banker GA (1988) Polarity orientation of microtubules in hippocampal neurons: uniformity in the axon and nonuniformity in the dendrite. *Proc Natl Acad Sci USA* 85: 8335 – 8339

Barkus RV, Klyachko O, Horiuchi D, Dickson BJ, Saxton WM (2008) Identification of an axonal kinesin-3 motor for fast anterograde vesicle transport that facilitates retrograde transport of neuropeptides. *Mol Biol Cell* 19: 274 – 283

Bechstedt S, Brouhard GJ (2012) Doublecortin recognizes the 13-protofilament microtubule cooperatively and tracks microtubule ends. *Dev Cell* 23: 181 – 192

Dotti CG, Sullivan CA, Banker GA (1988) The establishment of polarity by hippocampal neurons in culture. *J Neurosci* 8: 1454 – 1468

Farias GG, Cuitino L, Guo X, Ren X, Jarnik M, Mattera R, Bonifacino JS (2012) Signal-mediated, AP-1/clathrin-dependent sorting of transmembrane receptors to the somatodendritic domain of hippocampal neurons. *Neuron* 75: 810 – 823

Ferhat L, Cook C, Chauviere M, Harper M, Kress M, Lyons GE, Baas PW (1998) Expression of the mitotic motor protein Eg5 in postmitotic neurons: implications for neuronal development. *J Neurosci* 18: 7822 – 7835

Fourniol FJ, Sindelar CV, Amigues B, Clare DK, Thomas G, Perderiset M, Francis F, Houdusse A, Moores CA (2010) Template-free 13-protofilament microtubule-MAP assembly visualized at 8 A resolution. *J Cell Biol* 191: 463 – 470

Francis F, Koulakoff A, Boucher D, Chafey P, Schaar B, Vinet MC, Friocourt G, McDonnell N, Reiner O, Kahn A, McConnell SK, Berwald-Netter Y, Denoulet P, Chelly J (1999) Doublecortin is a developmentally regulated, microtubule-associated protein expressed in migrating and differentiating neurons. *Neuron* 23: 247 – 256

Franker MA, Hoogenraad CC (2013) Microtubule-based transport – basic mechanisms, traffic rules and role in neurological pathogenesis. *J Cell Sci* 126: 2319 – 2329

Gleeson JG, Lin PT, Flanagan LA, Walsh CA (1999a) Doublecortin is a microtubule-associated protein and is expressed widely by migrating neurons. *Neuron* 23: 257 – 271

Gleeson JG, Minnerath SR, Fox JW, Allen KM, Luo RF, Hong SE, Berg MJ, Kuzniecky R, Reitnauer PJ, Borgatti R, Mira AP, Guerrini R, Holmes GL, Rooney CM, Berkovic S, Scheffer I, Cooper EC, Ricci S, Cusmai R, Crawford TO *et al* (1999b) Characterization of mutations in the gene doublecortin in patients with double cortex syndrome. *Ann Neurol* 45: 146 – 153

Guillaud L, Setou M, Hirokawa N (2003) KIF17 dynamics and regulation of NR2B trafficking in hippocampal neurons. *J Neurosci* 23: 131 – 140

Hammond JW, Cai D, Blasius TL, Li Z, Jiang Y, Jih GT, Meyhofer E, Verhey KJ (2009) Mammalian kinesin-3 motors are dimeric *in vivo* and move by processive motility upon release of autoinhibition. *PLoS Biol* 7: e72

Hirokawa N, Noda Y, Tanaka Y, Niwa S (2009) Kinesin superfamily motor proteins and intracellular transport. *Nat Rev Mol Cell Biol* 10: 682 – 696

Hirokawa N, Niwa S, Tanaka Y (2010) Molecular motors in neurons: transport mechanisms and roles in brain function, development, and disease. *Neuron* 68: 610 – 638

Hoogenraad CC, Wulf P, Schiefermeier N, Stepanova T, Galjart N, Small JV, Grosveld F, de Zeeuw CI, Akhmanova A (2003) Bicaudal D induces selective dynein-mediated microtubule minus end-directed transport. *EMBO J* 22: 6004 – 6015

Horch HW, Katz LC (2002) BDNF release from single cells elicits local dendritic growth in nearby neurons. *Nat Neurosci* 5: 1177 – 1184

Horton AC, Racz B, Monson EE, Lin AL, Weinberg RJ, Ehlers MD (2005) Polarized secretory trafficking directs cargo for asymmetric dendrite growth and morphogenesis. *Neuron* 48: 757 – 771

Huang CF, Banker G (2012) The translocation selectivity of the kinesins that mediate neuronal organelle transport. *Traffic* 13: 549 – 564

Huber G, Matus A (1984) Differences in the cellular distributions of two microtubule-associated proteins, MAP1 and MAP2, in rat brain. *J Neurosci* 4: 151 – 160

Ikegami K, Heier RL, Taruishi M, Takagi H, Mukai M, Shimma S, Taira S, Hatanaka K, Morone N, Yao I, Campbell PK, Yuasa S, Janke C, Macgregor GR, Setou M (2007) Loss of alpha-tubulin polyglutamylation in ROSA22 mice is associated with abnormal targeting of KIF1A and modulated synaptic function. *Proc Natl Acad Sci USA* 104: 3213 – 3218

Jacobson C, Schnapp B, Banker GA (2006) A change in the selective translocation of the Kinesin-1 motor domain marks the initial specification of the axon. *Neuron* 49: 797 – 804

Janke C, Kneussel M (2010) Tubulin post-translational modifications: encoding functions on the neuronal microtubule cytoskeleton. *Trends Neurosci* 33: 362 – 372

Janke C (2014) The tubulin code: molecular components, readout mechanisms, and functions. *J Cell Biol* 206: 461 – 472

Jaworski J, Kapitein LC, Gouveia SM, Dortland BR, Wulf PS, Grigoriev I, Camera P, Spangler SA, Di Stefano P, Demmers J, Krugers H, Defilippi P, Akhmanova A, Hoogenraad CC (2009) Dynamic microtubules regulate dendritic spine morphology and synaptic plasticity. *Neuron* 61: 85 – 100

Kapitein LC, Schlager MA, Kuijpers M, Wulf PS, van Spronsen M, MacKintosh FC, Hoogenraad CC (2010a) Mixed microtubules steer dynein-driven cargo transport into dendrites. *Curr Biol* 20: 290 – 299

Kapitein LC, Schlager MA, van der Zwan WA, Wulf PS, Keijzer N, Hoogenraad CC (2010b) Probing intracellular motor protein activity using an inducible cargo trafficking assay. *Biophys J* 99: 2143 – 2152

Kapitein LC, Hoogenraad CC (2011) Which way to go? Cytoskeletal organization and polarized transport in neurons. *Mol Cell Neurosci* 46: 9 – 20

Kapitein LC, Yau KW, Gouveia SM, van der Zwan WA, Wulf PS, Keijzer N, Demmers J, Jaworski J, Akhmanova A, Hoogenraad CC (2011) NMDA receptor activation suppresses microtubule growth and spine entry. *J Neurosci* 31: 8194 – 8209

Kim MH, Cierpicki T, Derewenda U, Krowarsch D, Feng Y, Devedjiev Y, Dauter Z, Walsh CA, Otlewski J, Bushweller JH, Derewenda ZS (2003) The DCX-domain tandems of doublecortin and doublecortin-like kinase. *Nat Struct Biol* 10: 324 – 333

Kim T, Gondre-Lewis MC, Arnaoutova I, Loh YP (2006) Dense-core secretory granule biogenesis. *Physiology* 21: 124 – 133

Lawrence CJ, Dawe RK, Christie KR, Cleveland DW, Dawson SC, Endow SA, Goldstein LS, Goodson HV, Hirokawa N, Howard J, Malmberg RL, McIntosh JR, Miki H, Mitchison TJ, Okada Y, Reddy AS, Saxton WM, Schliwa M, Scholey JM, Vale RD *et al* (2004) A standardized kinesin nomenclature. *J Cell Biol* 167: 19 – 22

Lazo OM, Gonzalez A, Ascano M, Kuruvilla R, Couve A, Bronfman FC (2013) BDNF regulates Rab11-mediated recycling endosome dynamics to induce dendritic branching. *J Neurosci* 33: 6112 – 6122

Liu JS, Schubert CR, Fu X, Fourniol FJ, Jaiswal JK, Houdusse A, Stultz CM, Moores CA, Walsh CA (2012) Molecular basis for specific regulation of neuronal kinesin-3 motors by doublecortin family proteins. *Mol Cell* 47: 707 – 721

Lo KY, Kuzmin A, Unger SM, Petersen JD, Silverman MA (2011) KIF1A is the primary anterograde motor protein required for the axonal transport of dense-core vesicles in cultured hippocampal neurons. *Neurosci Lett* 491: 168 – 173

Lochner JE, Spangler E, Chavarha M, Jacobs C, McAllister K, Schuttner LC, Scalettar BA (2008) Efficient copackaging and cotransport yields postsynaptic colocalization of neuromodulators associated with synaptic plasticity. *Dev Neurobiol* 68: 1243 – 1256

Millecamps S, Julien JP (2013) Axonal transport deficits and neurodegenerative diseases. *Nat Rev* 14: 161 – 176

Nakata T, Hirokawa N (2003) Microtubules provide directional cues for polarized axonal transport through interaction with kinesin motor head. *J Cell Biol* 162: 1045 – 1055

Ou CY, Poon VY, Maeder CI, Watanabe S, Lehrman EK, Fu AK, Park M, Fu WY, Jorgensen EM, Ip NY, Shen K (2010) Two cyclin-dependent kinase pathways are essential for polarized trafficking of presynaptic components. *Cell* 141: 846 – 858

Quassollo G, Wojnacki J, Salas DA, Gastaldi L, Marzolo MP, Conde C, Bisbal M, Couve A, Caceres A (2015) A RhoA signaling pathway regulates dendritic Golgi outpost formation. *Curr Biol* 25: 971 – 982

Rolls MM (2011) Neuronal polarity in Drosophila: sorting out axons and dendrites. *Dev Neurobiol* 71: 419 – 429

Schlager MA, Hoogenraad CC (2009) Basic mechanisms for recognition and transport of synaptic cargos. *Mol Brain* 2: 25

Schlager MA, Kapitein LC, Grigoriev I, Burzynski GM, Wulf PS, Keijzer N, de Graaff E, Fukuda M, Shepherd IT, Akhmanova A, Hoogenraad CC (2010) Pericentrosomal targeting of Rab6 secretory vesicles by Bicaudal-D-related protein 1 (BICDR-1) regulates neuritogenesis. *EMBO J* 29: 1637 – 1651

Schlager MA, Serra-Marques A, Grigoriev I, Gumy LF, Esteves da Silva M, Wulf PS, Akhmanova A, Hoogenraad CC (2014) Bicaudal d family adaptor proteins control the velocity of Dynein-based movements. *Cell Rep* 8: 1248 – 1256

Shin E, Kashiwagi Y, Kuriu T, Iwasaki H, Tanaka T, Koizumi H, Gleeson JG, Okabe S (2013) Doublecortin-like kinase enhances dendritic remodelling and negatively regulates synapse maturation. *Nat Commun* 4: 1440

Sirajuddin M, Rice LM, Vale RD (2014) Regulation of microtubule motors by tubulin isotypes and post-translational modifications. *Nat Cell Biol* 16: 335 – 344

van Spronsen M, Mikhaylova M, Lipka J, Schlager MA, van den Heuvel DJ, Kuijpers M, Wulf PS, Keijzer N, Demmers J, Kapitein LC, Jaarsma D, Gerritsen HC, Akhmanova A, Hoogenraad CC (2013a) TRAK/Milton motor-adaptor proteins steer mitochondrial trafficking to axons and dendrites. *Neuron* 77: 485 – 502

van Spronsen M, van Battum EY, Kuijpers M, Vangoor VR, Rietman ML, Pothof J, Gumy LF, van Ijcken WF, Akhmanova A, Pasterkamp RJ, Hoogenraad CC (2013b) Developmental and activity-dependent miRNA expression profiling in primary hippocampal neuron cultures. *PLoS ONE* 8: e74907

Stepanova T, Slemmer J, Hoogenraad CC, Lansbergen G, Dortland B, De Zeeuw CI, Grosveld F, van Cappellen G, Akhmanova A, Galjart N (2003) Visualization of microtubule growth in cultured neurons via the use of

EB3-GFP (end-binding protein 3-green fluorescent protein). *J Neurosci* 23: 2655 – 2664

Stiess M, Bradke F (2011) Neuronal polarization: the cytoskeleton leads the way. *Dev Neurobiol* 71: 430 – 444

Szebenyi G, Bollati F, Bisbal M, Sheridan S, Faas L, Wray R, Haferkamp S, Nguyen S, Caceres A, Brady ST (2005) Activity-driven dendritic remodeling requires microtubule-associated protein 1A. *Curr Biol* 15: 1820 – 1826

Tanaka T, Serneo FF, Higgins C, Gambello MJ, Wynshaw-Boris A, Gleeson JG (2004) Lis1 and doublecortin function with dynein to mediate coupling of the nucleus to the centrosome in neuronal migration. *J Cell Biol* 165: 709 – 721

Tortosa E, Galjart N, Avila J, Sayas CL (2013) MAP1B regulates microtubule dynamics by sequestering EB1/3 in the cytosol of developing neuronal cells. *EMBO J* 32: 1293 – 1306

van der Vaart B, van Riel WE, Doodhi H, Kevenaar JT, Katrukha EA, Gumy L, Bouchet BP, Grigoriev I, Spangler SA, Yu KL, Wulf PS, Wu J, Lansbergen G, van Battum EY, Pasterkamp RJ, Mimori-Kiyosue Y, Demmers J, Olieric N, Maly IV, Hoogenraad CC *et al* (2013) CFEOM1-associated kinesin KIF21A is a cortical microtubule growth inhibitor. *Dev Cell* 27: 145 – 160

Walczak CE, Gayek S, Ohi R (2013) Microtubule-depolymerizing kinesins. *Annu Rev Cell Dev Biol* 29: 417 – 441

Watanabe K, Al-Bassam S, Miyazaki Y, Wandless TJ, Webster P, Arnold DB (2012) Networks of polarized actin filaments in the axon initial segment provide a mechanism for sorting axonal and dendritic proteins. *Cell Rep* 2: 1546 – 1553

de Wit J, Toonen RF, Verhaagen J, Verhage M (2006) Vesicular trafficking of semaphorin 3A is activity-dependent and differs between axons and dendrites. *Traffic* 7: 1060 – 1077

Witte H, Neukirchen D, Bradke F (2008) Microtubule stabilization specifies initial neuronal polarization. *J Cell Biol* 180: 619 – 632

Yau KW, van Beuningen SF, Cunha-Ferreira I, Cloin BM, van Battum EY, Will L, Schatzle P, Tas RP, van Krugten J, Katrukha EA, Jiang K, Wulf PS, Mikhaylova M, Harterink M, Pasterkamp RJ, Akhmanova A, Kapitein LC, Hoogenraad CC (2014) Microtubule minus-end binding protein CAMSAP2 controls axon specification and dendrite development. *Neuron* 82: 1058 – 1073

Ye B, Zhang Y, Song W, Younger SH, Jan LY, Jan YN (2007) Growing dendrites and axons differ in their reliance on the secretory pathway. *Cell* 130: 717 – 729

Zahn TR, Angleson JK, MacMorris MA, Domke E, Hutton JF, Schwartz C, Hutton JC (2004) Dense core vesicle dynamics in *Caenorhabditis elegans* neurons and the role of kinesin UNC-104. *Traffic* 5: 544 – 559

Zheng Y, Wildonger J, Ye B, Zhang Y, Kita A, Younger SH, Zimmerman S, Jan LY, Jan YN (2008) Dynein is required for polarized dendritic transport and uniform microtubule orientation in axons. *Nat Cell Biol* 10: 1172 – 1180

